Colloid Polym Sci 276:483–495 (1998)


ORIGINAL CONTRIBUTION

F. Dan
C. Vasiliu-Oprea

# Anionic polymerization of caprolactam in organic media. Morphological aspects

Received: 1 August 1997
Accepted: 5 February 1998

F. Dan · C. Vasiliu-Oprea (✉)
Department of Macromolecules
"Gh. Asachi" Technical University
6600 Iasi
Romania

**Abstract** Crystalline entities formed during anionic polymerization of caprolactam (CL) in nonpolar solvents were examined, mainly by scanning electron microscopy and wide angle X-ray scattering. The morphological development of these entities is governed by the complex interaction between the competing polymerization and physical processes like phase separation and crystallization. The effect of the efficiency of catalytic systems on their interaction, the mechanisms of the phase separation and the crystal growth under topological restrictions set by the phase separation are discussed. Under reaction conditions, for these ones favouring high polymer yields, the final morphology of the polycaproamide (PCA) particles can be controlled by the efficiency of both catalytic species (activator and catalyst). Despite the large range of particle sizes two typical morphologies, namely – connected globules evolving to large blocks and macroporous powders are obtained using more or less efficient catalytic systems, respectively. An adequate selection of the catalytic pairs allows to control the particles' size and their internal morphology, which is important for certain specific applications of PCA.

**Key words** Anionic polymerization of caprolactam in solvents – polymerization induced phase separation – efficiency of catalytic system – macroporous powders – fused agglomerates

## Introduction

This paper is concerned with the formation and morphological development of PCA particles formed by anionic polymerization of caprolactam (CL) in nonpolar solvents.

The anionic polymerization of CL in solvents is a convenient process because it occurs with high rates at temperatures well below the melting point of PCA and leads to high molecular weight polycaproamide, characterized by high molecular homogeneity in the form of fine dispersion [1]. This form facilitates its purification easily and is very suitable for different processing procedures, such as flame spraying, electrostatic coating, paste production, dispersions and lacquer binders, techniques of spinning, to give filaments, and of dyeing. Polycaproamide (PCA) particles thus obtained are crystalline entities and their shape and size are influenced by the synthesis parameters, e.g. nature of solvent, monomer/solvent ratio, temperature, stirring rate, and the type, concentration and the ratio of catalytic components. Although, this process is well known for many years [2] neither the typical morphologies nor the link between these morphologies and the parameters mentioned above have been investigated in detail. A literature survey reveals the influence of one or more of these factors on the morphology of PCA-particles. Using different catalytic systems and/or solvents, PCA-particles with sizes varying from a few microns to more than 1 mm have been

obtained [3–12]. Usually, the formation of particles has been associated with polymer precipitation, which occurs during the polymer synthesis. However, taking into account the variety of the morphologies obtained, an alternate route involving the occurrence of liquid–liquid, and liquid–crystal phase separation might be considered. Early work in polymer solution crystallization proved that both kinds of phase separation could occur in poor solvents [13]. A high activation energy is needed for crystallization and usually liquid–liquid demixing will precede solid–liquid demixing even if solid–liquid demixing is favored thermodynamically [14, 15]. In addition, the deformation of polymer chains under the shear field, which usually accompanies the polymerization in solution, effectively shifts the binodal to higher temperatures, allowing liquid–liquid-phase separation to occur [16].

In the present paper, a more detailed analysis of the interaction between the competing polymerization and phase separation processes on the morphology of PCA particles is presented. An emphasis is placed on the influence of the catalytic system (its efficiency) on the interaction between the chemical and phase-separation processes. The findings are discussed by comparing with those obtained in systems, such as thermally induced phase separation and ternary systems polymer/solvent/nonsolvent. The analysis of the resulting morphologies may be a useful tool not only in understanding the competition between chemical and physical processes involved here, but it can also give some qualitative information about the relative efficiency of the different catalytic systems.

## Experimental

### Materials

RedAl® 3.5 M solution of sodium *bis*-(2-methoxyethoxy) aluminium hydride in toluene (Fluka), isophorone diisocyanate (IDI) (Aldrich), hexamethylene diisocyanate (HDI) (Fluka), 2,2,4-trimethylhexamethylene diisocyanate (THDI), *N*,*N*′-diisopropylcarbodiimide (DICI), and *N*,*N*′-dicyclohexylcarbodiimide (DCCI) (Fluka) were used as received.

*N*-acetylcaprolactam (NAcCL) was prepared, according to the literature [17], by heating equimolar amounts of acetic anhydride and CL in benzene to reflux followed by vacuum distillation (b.p. 125–126 °C/17 mm, $n_D^{20} = 1.4890$).

The purification of caprolactam (technical grade, Fibrex S.A. Savinesti, Romania) and of ethylbenzene was described elsewhere [10]. Carbon dioxide ($CO_2$) was purified by passing it through concentrated sulfuric acid and phosphorus pentoxide deposited on glass wool.

### Polymerization

The polymerization prodedure and the workup of polymers were detailed in our previous papers [10, 12]. Sodium caprolactamate (NaCL) or sodium dicaprolactam-*bis*(2-methoxyethoxy) aluminate (RedNaCL) catalysts were prepared at 77 °C, by reacting CL with metallic sodium (the exact amount of sodium was measured by extruding a thin cylindrical piece of metal through a calibrated glass tube) or with RedAl (pipetting the required volume), respectively. When the reactions were completed – as indicated by complete dissolution of metallic sodium and cessation of hydrogen formation – the temperature was quickly raised to 130 °C and the reaction mixture was equilibrated at this temperature. At the reaction temperature, the activators were added under nitrogen and stirred. The flow of nitrogen was stopped and a continuous stream of $CO_2$, used as activator for part of the experiments, was passed through the solution at a rate of 30 ml/min. The moment at which active compounds were added was considered as "zero" time of polymerization. The polymerization conditions are given in Table 1.

### Characterization methods

All characterizations, i.e. polymer yield, particle size distribution, mercury porosimetry, SEM photos, and WAX-curves, were performed by following the already described methods [10, 12].

## Results and discussion

### Polymerization

Anionic polymerization of CL occurs by the activated monomer mechanism [19]. The propagation, occurring by a two-step mechanism, involves the acylation of the lactam anion by the *N*-acyllactam end-group, followed by fast proton-exchange with monomer:

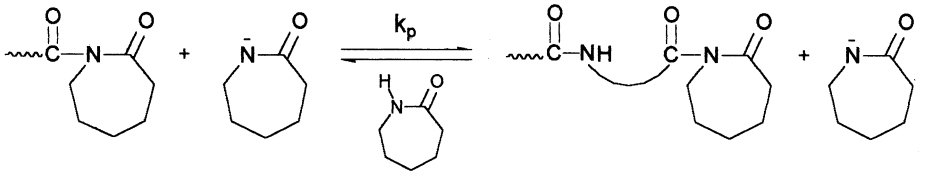


(1)

The result of the above reactions is the incorporation of one linear monomer unit into the polymer chain and regeneration of both active species.

The high rate of anionic polymerization is due to the fact that both reacting species are highly reactive: the activated monomer, i.e. lactam anion, with increased nucleophilicity and the growth centre, i.e. *N*-acyllactam group, with enhanced acylating ability [20].

The overall process is influenced by the initiation step. The initiation is related to the absence of the *N*-acyllactam groups at the beginning of polymerization. Consequently, the following two limiting situations are possible: (a) acylation of the lactam anion by the lactam monomer (self-initiation or non-activated polymerization); and (b) use of preformed *N*-acyllactams or their precursors (acyl halides, anhydrides and isocyanates). In the case (a), the formation of *N*-acyllactam groups (i.e. "tadpole form" dimer, structure (**1**) occurs slowly because the lactams are moderately efficient acylating agents and a considerable induction period characterizes the self-initiation. Instead, using the preformed *N*-acyllactams (structure (**2**)) of at least the same reactivity as *N*-acyllactams chain-end, polymerization starts directly with the propagation reaction.

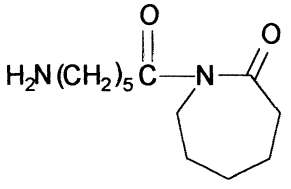

( **1** )

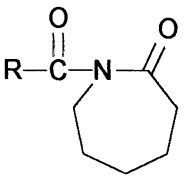

( **2** )

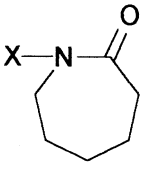

( **3** )

Between the two boundaries, the length of the induction period can be controlled by a suitable choice of activating compounds. Several classes of reactants are able to activate the polymerization. These reactants can be divided into two main groups depending on the provenience of the acyl residue of *N*-acyllactam initiating species, namely from the activating compound or from the polymerizing lactam. The first group is derived from less reactive (towards lactam or its anion) acylating compounds such as esters, lactones, and amides. The second one comprises substances with the general structure (**3**) (or theirs precursors) such as: *N*-acylamidines, ketene imines, organophosphorus lactams, alkylsilyl lactams, imino chlorides, etc. [21]. The common feature of all these activating compounds is that at least two stages of initiation are required to produce the true initiating species [22].

The use of different catalytic systems to control the morphological development of PCA particles has the advantage that all the other parameters of synthesis can be kept at their optimal values with respect to polymer yield and degree of polymerization. Throughout this work, the conditions for the synthesis (except for the nature of catalytic components) were kept identical.

In Table 1 the data concerning the efficiency of catalytic systems, the course of polymerization, and the final morphology are given. For the sake of simplicity, we qualitatively divided both catalytic species in two main classes, namely quick and slow, in accordance with their effect on the overall rate of polymerization. Thus, taking into account the above classification of activators, quick activators are all compounds able to suppress the induction period (i.e. preformed *N*-acyllactams or their precursors, which react fast with CL). All other activating compounds are designed as slow activators and in this case, the initiation is the rate-determining step of polymerization. The catalysts are classified in accordance with their relative nucleophilicity. Thus, caprolactamates of alkali metals are referred to as quick and those obtained by reacting CL with alkali metal aluminium alcolates are considered as slow catalysts, respectively. It is believed that the last catalysts, with electron-donating substituents, decrease the nucleophilicity of the lactam anion by coordinating the aluminate with the lactam carbonyl oxygen to effectively delocalize the negative charge, structure (**4**) [23]:

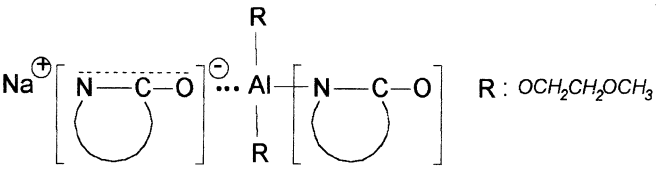

( **4** )

The slower reaction of this reduced activated monomer with the *N*-acyllactam affects the reaction rate. Retardation of this reaction was also ascribed to side reactions that occur in the reaction medium, giving rise to 2-methoxyethanol [24] and to a certain measure to hexamethyleneimine, both strong inhibitors of anionic polymerization.

**Table 1** Influence of the catalytic system on the separation time of polymer, $t_s$, polymer yield, and particle size[a)]

| Code | Cat. | Act. | Time [min] | Yield[b)] | $t_s$[c)] [s] | Particles | |
|---|---|---|---|---|---|---|---|
| | | | | | | Shape | Size [$\mu$m] |
| a0 | Na (met.) | NAcCL | 20 | 90.5 | 8 | B | — |
| a1 | Na | HDI | 20 | 94 | 10 | B | — |
| a10[d)] | Na | HDI | 60 | 8.7 | 5 | FA | 4–60 |
| a11[e)] | Na | HDI | 40 | 87.5 | 48 | FA | 200–1600 |
| a12[e)] | Na | HDI | 40 | 76.4 | 76 | FA | 100–800 |
| b1 | RedAl | HDI | 20 | 54.6 | 53 | FA | 900–1500 |
| b2 | RedAl | THDI | 20 | 64.7 | 61 | FA | 600–1000 |
| b3 | RedAl | IDI | 20 | 73.5 | 72 | FA | 150–600 |
| c1 | Na | $CO_2$[f)] | 30 | 44 | 162 | FP | 2.8–21 |
| c2 | Na | DICI | 40 | 55 | 354 | P | 18–210 |
| c3 | Na | DCCI | 40 | 58 | 417 | P | 30–285 |
| d1 | RedAl | DICI | 60 | 48 | 598 | P | 16–190 |
| d2 | RedAl | DCCI | 60 | 53 | 670 | P | 30–225 |

*Abbreviations*: B, blocks; FA, fussed agglomerates (granules); P, powders; and FP, fine powders.
[a)] Reaction conditions: solvent, ethylbenzene (EB); temperature, 130–135°C; initial concentration of CL-3 mol/l; catalyst concentration, 3.3–3.5% mol/mol CL; activator/initiator ratio, 1 [eq. N-acylCL/mol catalyst].
[b)] Calculated from conversion of CL into polymer.
[c)] The period of time between the starting of polymerization and the moment when the reaction medium becomes translucent.
[d)] Polymerization temperature, 40 °C.
[e)] Concentration of 2-pyrrolidone, 1.7 and 3.4% mol/mol CL for samples a11 and a12, respectively.
[f)] Catalyst concentration, 7.0 mol%/mol CL.

Consequently, four situations are expected depending on the pairs of active species used to promote the polymerization, i.e. (a) quick–quick; (b) quick–slow; (c) slow–quick; and (d) slow–slow activator/catalyst pairs, respectively. The first letter from the sample designation code in Table 1, indicates in order the above presented pairs.

As expected, using quick–quick catalytic combinations, the time needed for phase separation to occur, $t_s$, is very short. In addition, the polymer yields approach those obtained in bulk polymerization. On the contrary, phase separation occurs after a long period and low conversions are obtained using slow–slow and slow–quick activator/catalyst systems. An intermediate position seems to characterize the quick–slow pairs.

The above-mentioned differences have to be related to the effect of the efficiency of the catalytic system on the competition between chemical and phase-separation processes. Under a given set of reaction conditions, the overall polymerization rate decreases with decreasing catalytic efficiency. A low ratio of initiation and propagation rate favours fast decay of catalytic components due to side reactions. Unlike the polymerization rate, the catalytic system efficiency does not directly affect the kinetics of physical processes. In this case, the physical termination [25], implying the occlusion of the acyllactam-type chain ends and of linear amide anions inside the polymer crystalline phase, is expected due to low reaction temperatures and the presence of a poor solvent. Conversely, at high ratios of initiation and propagation rate both the consumption of the catalytic species and the physical termination can be limited allowing to obtain high polymer yields.

## Morphology

Table 1 shows that the polymer morphology is strongly affected by the efficiency of the catalytic system. Polymer particles with sizes varying in a very large range, from blocks to fine powders have been obtained. However, it appears that PCA particles obtained using activator/catalyst pairs having similar efficiencies present similar morphologies.

### Quick–slow activator/catalyst systems

The typical morphologies obtained using these catalytic systems are described first because of their intermediate position with respect to both the efficiency of the catalytic system and the average size of the obtained particles.

In all experiments, irregularly shaped granules with a great variation of size and length/diameter ratio were

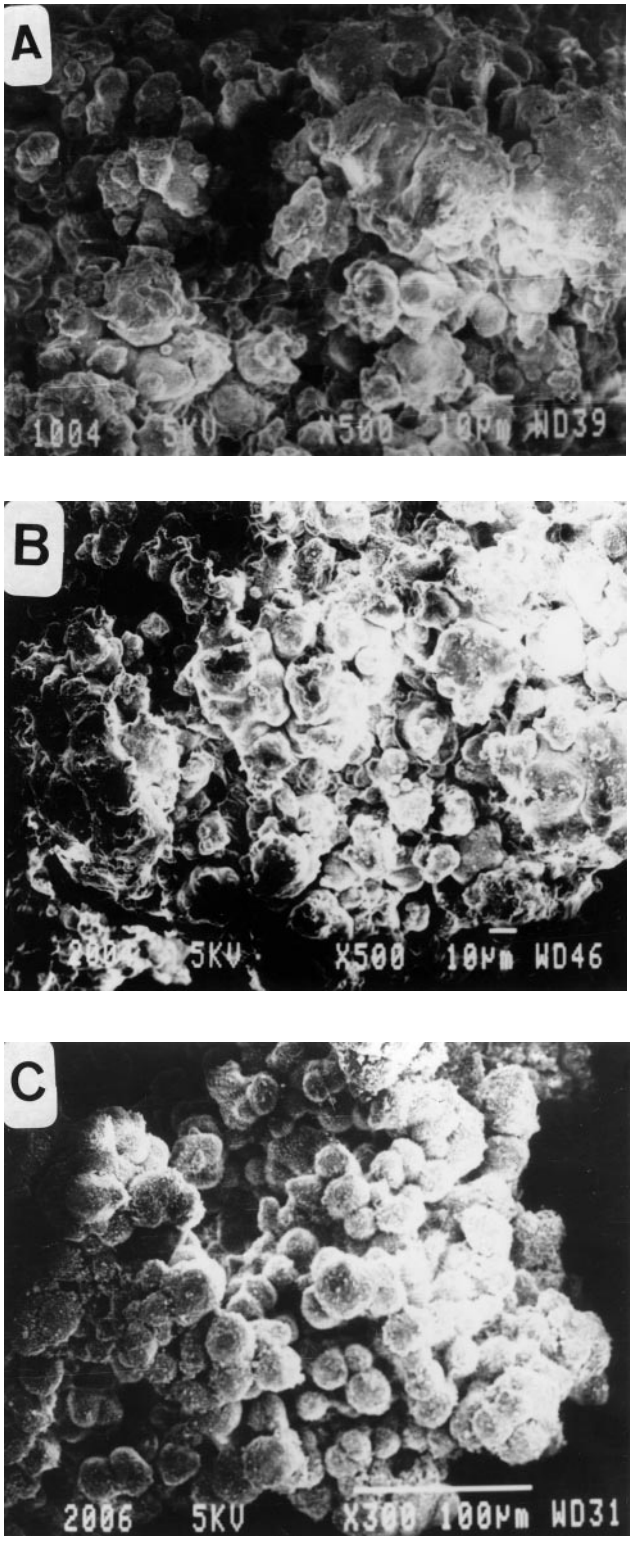


**Fig. 1** Low magnification of PCA granules showing the change of shape and size of the primary particles, from an irregular shape with broad distribution to an approximate spherical one concomitantly with decreasing activator efficiency. In Figs. 1–3 micrographs (A), (B) and (C) correspond to the samples b1, b2 and b3 in Table 1

obtained. However, in spite of these differences the granules have the same morphology, namely fused agglomerates of a great number of small individual particles, as is shown in Figs. 1A–C.

Using the same catalyst the chemical structure of the activator (its efficiency) affects the granule sizes even if the activators belong to the same chemical class [11], e.g. aliphatic diisocyanates (samples b1–b3 in Table 1). Thus, concomitantly with increasing activator efficiency (i.e. decreasing the time of polymer separation) the average size of granules increases (see Table 1).

In addition, the irregular shape of the individual particles in the granules changes into a more regular one with decreasing activator efficiency. Using more efficient activators, the polymerization occurs faster increasing both the polymer concentration in the reaction medium and the number of polymer-rich domains. This favors the coalescence of liquid droplets giving rise to bigger irregular particles, with a cactus-like structure, as shown in Figs. 2A and B.

Not only the size and external shape but also the inner structure of the particles forming the aggregates is affected by the activator efficiency. Figures 3A–C show that the morphology of individual particles gradually changes, passing from well-developed spherulitic structures to roughly spherical globules when the activators used were HDI, THDI, and IDI, respectively. Well-developed three dimensionally spherulitic structures, with lamellae radiating along the spherulite radius and having a densely packed core and an open morphology towards the periphery, are shown in Figs. 2A and 3A. Figure 3B also displays the less-developed lamellae or stacks of lamellae sticking out of the surface of the individual particles which compose the PCA-THDI granules. In both cases, it seems that a quantity of the polymer is transferred from the homogeneous medium to the already separated polymer. The growing chains, which appear at different moments in the homogeneous medium, are captured by the existing particles and form lamellae by direct deposition from the solution. Consequently, these morphologies do not totaly reflect the liquid–liquid phase separation that takes place during polymerization.

As is seen in the inset of Fig. 3C, through mechanical dispersion of the PCA-IDI granules the individual particles (globules) can be easily distinguished Schaaf et al. [26] suggested that the globules could be obtained more easily than single crystals from most crystallizable polymers, especially from those that are the least soluble. The globules are hard and dense, characterized by a low porosity, a very small number of them being broken by mechanical dispersion. The majority are roughly spherical, with diameters in range of 2–20 $\mu$m, and a relatively small number have irregular shapes. Figure 3C shows a

Colloid & Polymer Science, Vol. 276, No. 6 (1998)


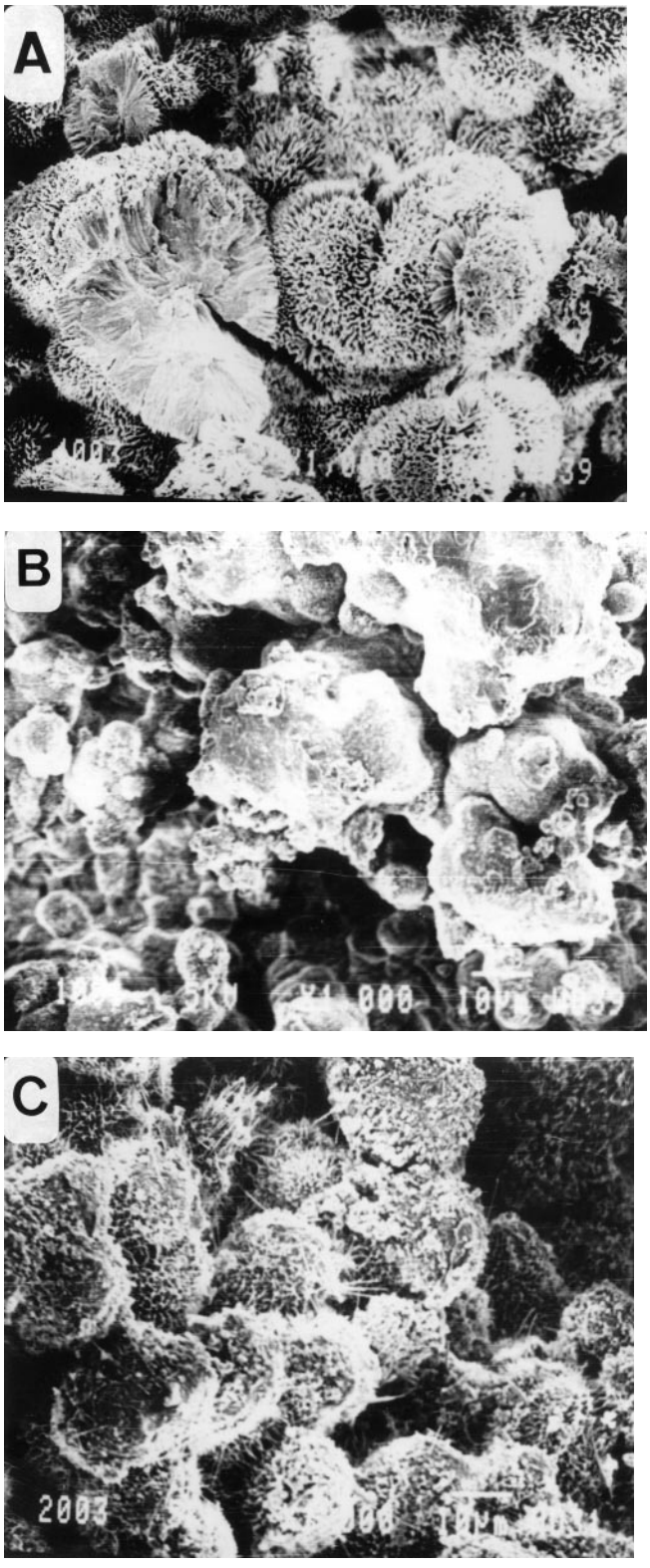


**Fig. 2** Medium magnification of the individual particles composing the granules showing the alteration of their structure, from a well-developed spherulitic structure to a compact and dense globular one, concomitantly with decreasing activator efficiency

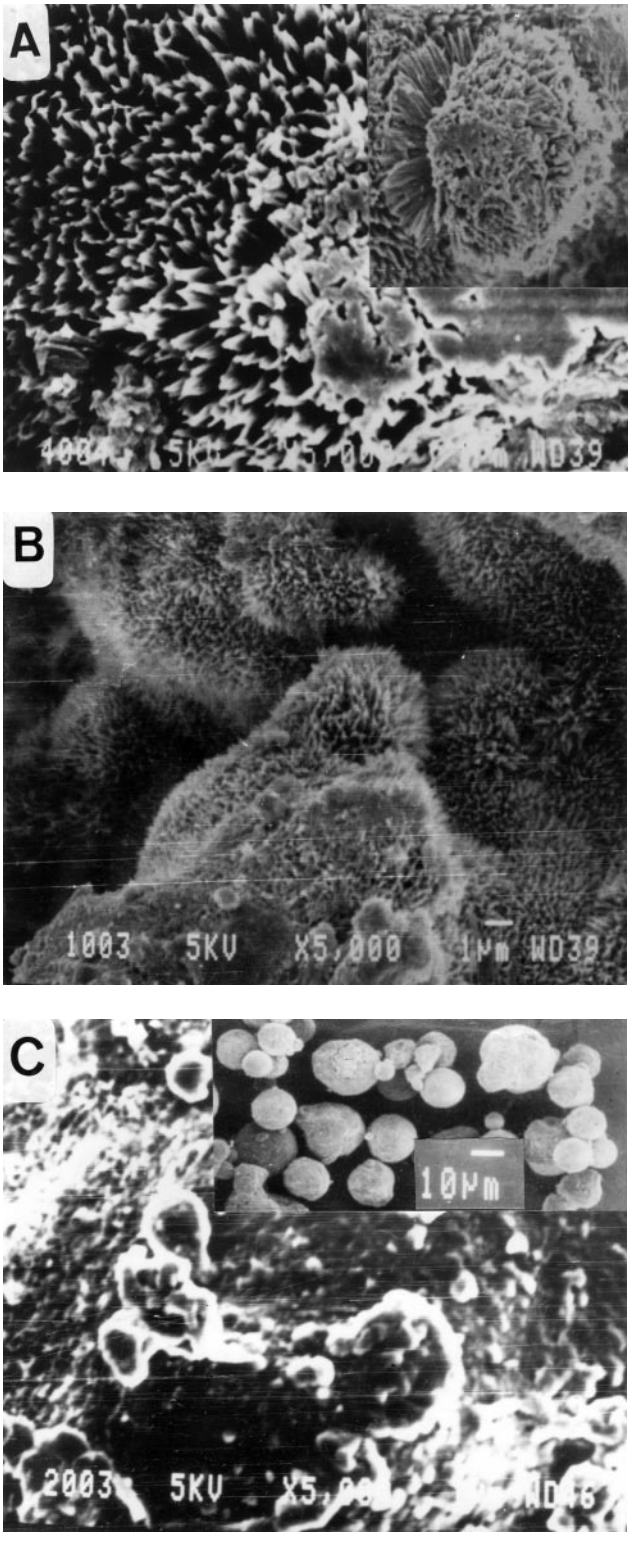


**Fig. 3** High magnification of the individual particles, which compose PCA granules, showing details of the external surface. In the insets a three dimensional spherulite (A) and a general view of the individualised globules, obtained through mechanical dispersion, (C) are presented

magnified section of the surface of PCA-IDI granules. It reveals a great number of agglomerates especially small globules. This morphology is achieved when small viscous globules touch an already solidified bigger globule. The spherical particles show a smooth external surface which is unusual for radial growth of polymer lamellae (Figs. 3A and B). In this case, it appears that the surface of droplets is the preferred nucleation and growth site.

Clearly, the shape of fused aggregates suggests the occurrence of a liquid–liquid phase separation. The initially homogeneous solution demixes after a period of time, $t_s$ (depending on the concentration of polymer and its degree of polymerization) into a polymer-rich phase and a solvent-rich phase. Most likely, the polymer-rich phase is in the form of liquid-like droplets [10]. At the very beginning of phase separation, separated translucent droplets can be visualized. After that, within a very short time, the aspect of the reaction medium suddenly changes due to chemical and physical processes involved. As the polymerization proceeds inside the droplets, the viscosity increases but also polymer crystallization is expected because of the undercooling. Under shear the droplets collide with each other, just before solidification occurs, giving rise to granules (fussed agglomerates).

The morphological differences found can not only be ascribed to the activator efficiency but also to the manner in which the growth of chains is started. Thus, when almost all chain initiator molecules start growing simultaneously, as probably in the case of IDI, the homogeneous solution demixes in more uniform domains. Because the reaction rate is relatively low there is enough time for the monomer to be transferred into the polymer-rich phase.

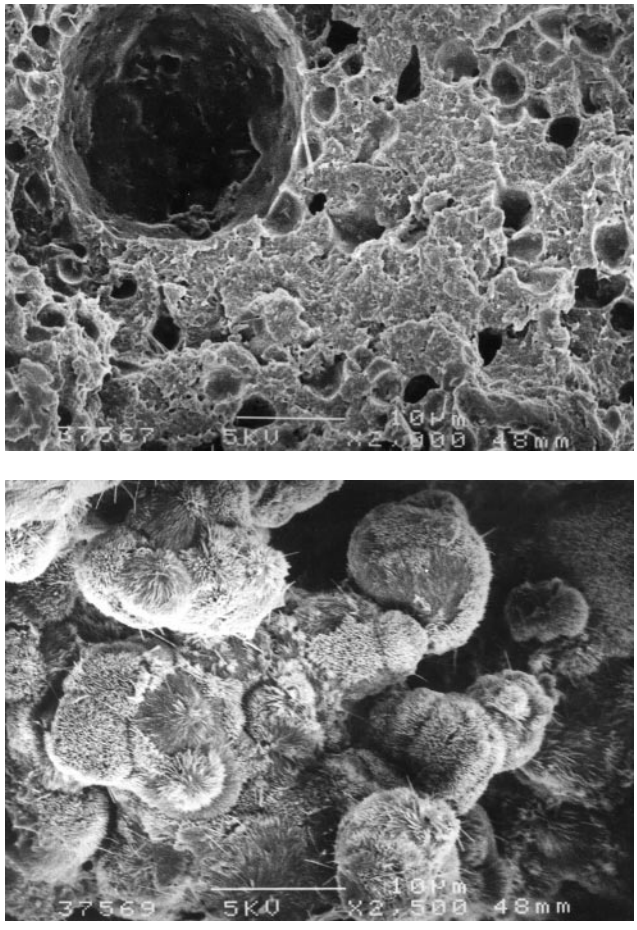


**Fig. 4** Scanning electron micrographs (sample a1 in Table 1) showing (A) the foam-like structure of the polymer deposited on the reaction flask walls and (B) PCA particles formed in the last stages of polymerization. Note the well developed spherulitic structure of PCA particles

## Quick-quick catalytic systems

Table 1 shows that in this case polymer yields are comparable with those obtained in anionic bulk polymerization and that phase separation occurs very quickly. Because some of the activators are the same as in the previous section, the differences can be related to the higher propagation rate. The enhanced lactamate nucleophilicity favours a rapid increase both of the degree of polymerization and polymer concentration. Even if translucent separated droplets can be seen, due to the high polymer concentration they rapidly collide. The coalescence continues forming larger and larger aggregates, which ultimately adhere to the walls of the reaction flask, Fig. 4A, or on the axle of the stirrer. A very small amount of polymer is obtained as particles, Fig. 4B. These probably appear in a late stage of polymerization when the monomer concentration in the reaction medium is low.

Decreasing the concentration of catalytic species and/or initial monomer concentration results in a drastic decrease in polymer yield but the morphology is not affected, i.e. in all cases the polymer was deposited on the walls of the reaction flask. This means that a high concentration of catalytic species is required to prevent the polymerization from being suppressed by side reactions and by physical termination. The only possibility to prevent deposition is to decrease the reaction temperature (sample a10 in Table 1). As expected, by decreasing the temperature the polymer yield also decreases (below 10% at 40 °C).

In order to verify whether the found morphological differences, between the two described classes, are related to the propagation rate, a new experiment was carried out by adding a small amount of 2-pyrrolidone to the reaction mixture. Using catalytic amounts of 2-pyrrolidone a decrease of the rate of propagation is expected because

2-pyrrolidone is more acidic and more reactive in the transacylation reactions (e.g. Eq. (2)) than caprolactam [27]:

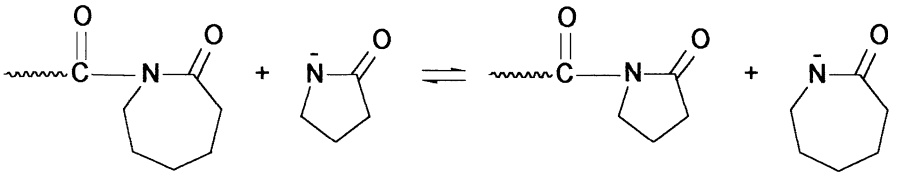

(2)

Indeed, in the presence of 2-pyrrolidone, granules (fused agglomerates) with sizes varying in a wide range and conversions between those obtained using NaCL and Red-NaCL as initiators, have been obtained (samples a11 and a12 in Table 1).

Slow-quick (and/or slow) catalytic systems

In these classes, the initiation is the rate-determining step of polymerization. Using the same catalyst (e.g. sodium, salt of caprolactam, NaCL) it is expected that not only the chemical structure of the activator but also the manner in which the growing centres are formed, i.e. instantaneously or stepwise, will influence the final morphology of particles. The investigated activating compounds form the active growing centres stepwise in the reaction medium and are able to act for varying periods as chain initiators. We suppose that the differences between the morphologies of PCA particles obtained in the presence of aliphatic diisocyanates and of those using less reactive compounds could be related to the above-mentioned pathways of growing centre formation.

Scanning electron micrographs of the PCA powders taken at low magnification (Figs. 5A and B) reveal that these particles do not result from an agglomeration process, as previously was described for the efficient catalytic systems. Under former reaction conditions, alwas-powdery particles were obtained. The finest powders were obtained when $CO_2$ was used as an activator. It suggests that the chain initiator species are faster generated in the reaction medium. In this case, the phase separation process appears to yield elongated flat "disk"-like irregular shaped powders, as is illustrated in Fig. 5A. The shape of the particles become more spherical with increasing $t_s$, i.e. when DCCI was used to activate the polymerization (Fig. 5B). As is seen in these figures, both the powders display a rough external structure. The solidified polymer forms a continuous structure giving the powder physical cohesion, while the solvent which fills the empty spaces forms a continuous liquid phase with the reaction medium.

Both the PCA-$CO_2$ and PCA-DCCI powders are highly porous (containing especially macropores), as is shown in Figs. 6A and B, respectively. As is seen in Table 2,

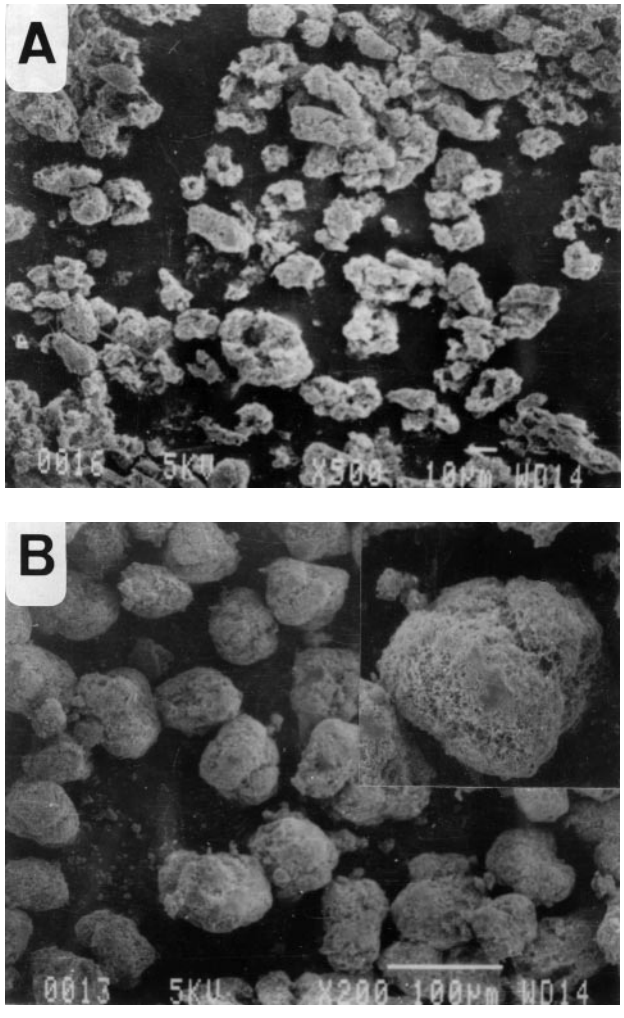


**Fig. 5** Low magnification scanning electron micrographs of the PCA powders (note that the powders do not represent fused aggregates). In the inset of (B) a closer view of an individual powder is presented. In Figs. 5 and 6 micrographs (A) and (B) correspond to the samples c1 and c3 in Table 1, respectively

PCA-$CO_2$ powders contain the lowest mesopore fraction (only 3.44% from the total pore volume) while PCA-DCCI powders contain the highest mesopore fraction (23.48%) [12]. The pore volume distribution of PCA-DICI is

**Table 2** Physical properties of PCA powders derived from BET and mercury intrusion methods

| Sample | BET area [$m^2/g$] | Total pore volume | | Porosity[a] [%] | Pore-size distribution[b] | |
|---|---|---|---|---|---|---|
| | | BET [$cm^3/g$] | Mercury intrusion [$cm^3/g$] | | Mesopores [%] | Macropores [%] |
| PCA-$CO_2$ | 5.8 | 1.37 | 1.45 | 77.7 | 3.44 | 96.56 |
| PCA-DICI | 3.19 | 0.75 | 1.06 | 66.3 | 8.27 | 91.73 |
| PCA-DCCI | 1.76 | 0.415 | 0.40 | 62.6 | 23.48 | 76.52 |

[a] Evaluated by equation: $P\% = (1 - d_a/d) \times 100\%$.
[b] macropores, $r > 25$ nm; mesopores, $1 < r > 25$ nm; and micropores, $r < 1$ nm [28].

intermediate between the two above-mentioned distributions. It appears that PCA-$CO_2$ powders have the highest pore volume as well as specific surface area. A more dense structure is characteristic for the PCA-$CO_2$ sample, as compared to the PCA-DCCI powders, even if their structure is similar, i.e. a connected network type. The network structure is a fibrillar one, with fibrils interconnected to each other. Some fibrils can also form bundles of fibrils and these could ensure "the resistance skeleton" of the whole particle. It is evident from Figs. 6A (inset) and 6B that both the individual fibrils and bundles of fibrils can be connected to two or more similar fibrils/bundles thus giving rise to the final network morphology.

Using these activating compounds, after the polymerization is started in the homogeneous medium the viscosity of the reaction mixture gradually increases, mainly due to the formation of salts of some of the products [29]. When the concentration of generated active centres (i.e. *N*-acyllactam groups) becomes significant, the growing of chains also occurs, and a faint opalescence appears indicating the occurrence of phase separation. The demixing process is initially dominated by liquid–liquid-phase separation forming polymer-rich and -poor regions. The connectivity of the polymer rich-phase is rapidly interrupted by shear forces and by an increase of the interfacial tension, resulting in droplet-type morphology. In this stage we can assume that each droplet has the consistency of a viscous semiliquid medium. Considering now the droplet itself as an isolated system, phase separation will proceed within each droplet. If the droplet has a composition, that a slight increase of polymer concentration is able to induce spinodal demixing, bicontinuous structures of both segregates phases are obtained. Because the reaction temperature is well below (about 70–80 °C) the melting point of the polymer, the polymer-rich phase will crystallize, and the phase separation process will be discontinued. The solidified polymer forms a continuous structure giving the powder physical cohesion, while the solvent which fills the empty spaces forms a continuous liquid phase with the reaction medium.

This does not mean that the chemical process is suppressed at least as long as the lactamate anions exist in the reaction medium. In this stage, new initiating molecules are gradually generated and the polymerization proceeds. Subsequently, there are three possible polmerization sites, namely in the homogeneous phase, inside of the particle,

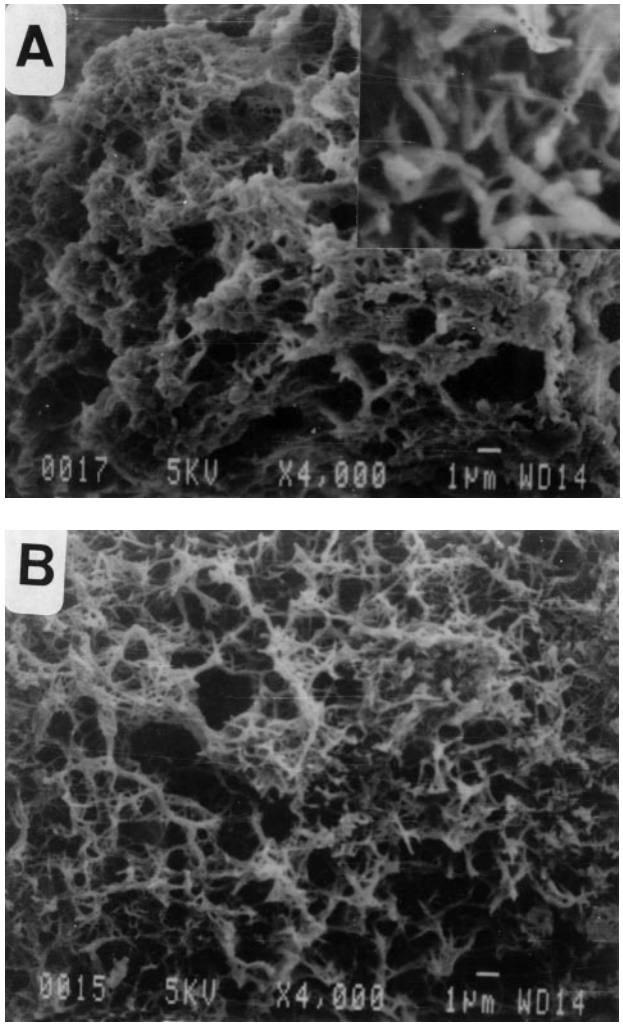


**Fig. 6** High magnification scanning electron micrographs of the PCA powders showing the macroporous structure (interconnected network). In the inset, a closer view, showing structural details, is presented

and on the surface of particles. Overall, polymerization is expected to proceed predominantly inside and at the surface of large particles, in concordance with the high porosity and extended surface of the powders and with the high affinity between the already separated polymer, monomer, and catalytic species. However, the polymerization reaction occurring in the homogeneous phase is not negligible. Most likely, a fraction of oligomeric chains, soluble in the reaction medium, is absorbed inside or on the surface of separated particles. In Figs. 5A and B two frequently observed deviations from the general shape of the powders, i.e. small particles and asymmetric powders can be identified. The competition between the growth of powders by the absorption of soluble growing chains onto pre-existing particles and the formation of new particles in the homogeneous medium, allows the formation of the observed small particles. When the soluble growing chains are absorbed on the external surface of particles, the subsequent polymerization may lead to asymmetric powders. The asymmetric powders or even double or triple particles (especially in the case of PCA-DCCI powders) may result from coalescence, when one particle is already solidified and another just segregates.

## Wide-angle X-ray diffraction

The crystalline structure of the PCA particles was investigated using WAXS. The X-ray intensity diffraction patterns, for PCA granules (quick-slow) and PCA powders (slow-quick) catalytic systems are depicted in Figs. 7A and B, respectively. All the investigated samples contains predominantly the $\alpha$ crystalline phase, a small fraction or $\gamma$ crystalline phase being also present. However, comparing these figures the differences in the shape of patterns are evident. It is clear that the efficiency of the catalytic system can influence both the morphology and the crystalline structure of PCA particles. Thus, the intensity of the peaks corresponding to the crystallographic plane $\alpha_2$(002, 202) is always stronger as compared to those corresponding to the crystallographic plane $\alpha_1$(200) when the polymerization was initiated using quick-slow activator/catalyst systems (PCA granules). Moreover, it should be noted that the intensity of the peaks in the $\alpha_1$(200) plane gradually decreases with increasing activator efficiency (i.e. in the case of more developed spherulitic structures). It seems that at high polymerization rates and in the presence of solvent the growth of crystals in the $\alpha_1$(200) plane could be retarded. In contrast, the X-ray diffraction patterns corresponding to PCA powders show that the intensity of the peaks in the crystallographic plane $\alpha_1$(200) is stronger than those from the crystallographic plane $\alpha_2$(002, 202). Also, the half width of the reflection peaks from the crystallographic plane $\alpha_1$(200) is lower as compared with the corresponding one from the plane $\alpha_2$(002, 202), i.e. a more perfect crystalline arrangement and larger crystals are developed in the direction perpendicular to the $\alpha_1$(200) plane.

There exists a physical relationship between the two peaks because both originate from the $\alpha$-phase crystals. In case of three-dimensional order, the intensities of the two peaks should be the same [30]. In the specific investigated systems, complex kinetic and rheological factors could induce small rotations of the unit cell around the normal to the plane 002, $N_{002}$ or around the normal to the plane 200, $N_{200}$, during the synthesis of PCA granules or powders, respectively.

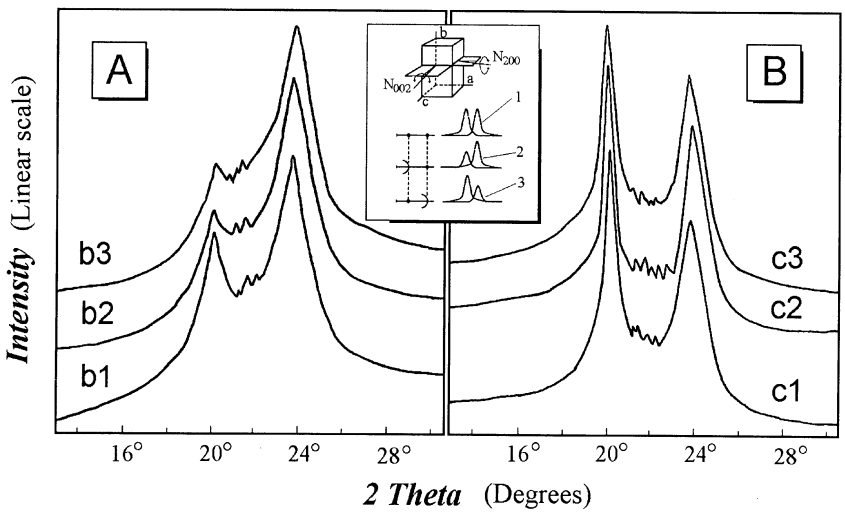


**Fig. 7** WAXS powder pattern; sample code refers to Table 1. (A) granular PCA; and (B) powdered PCA. In the inset, the effect of orientation on the ratio between the areas of two peaks is illustrated
1 – perfect orientation;
2 – rotation about $N_{002}$; and
3 – rotation about $N_{200}$

A general view

Anionic polymerization of CL in nonpolar solvents is a complex process. It combines the main features of the heterogeneous phase polymerization of lactams with some characteristic features of precipitation and/or dispersion polymerization of vinyl monomers. On the other hand, with respect to the physical processes, i.e. liquid–liquid phase separation and liquid–crystal transformation, the anionic polymerization of CL rather resembles the thermally induced phase separation of crystalline polymers in poor solvents.

To our knowledge all phenomena that occur during the anionic polymerization of CL can be best described in terms of polymerization-induced phase separation (PIPS). In the PIPS method, phase separation and polymerization occur simultaneously. The PIPS method has been mostly applied to polymer systems, such as polymer blends [31, 32] and polymer-dispersed liquid crystals (PDLCs) [33, 34]. Chan and Rey have theoretically studied the polymerization-induced phase separation in a monomer-solvent system [35]. Despite numerous differences at the molecular level, many quantitative similarities seem to be common among them.

A hypothetical phase diagram showing the expected boundary situations for the investigated system is presented in Fig. 8. Because in this figure the concentration, $C$ is taken to be the solvent volume fraction, the reaction point remains in the same place during polymerization, but it can be thrust in the unstable (or metastable) region of the phase diagram or can remain below the solid–liquid line. The phase separation processes that occur after the reaction point is moved in the miscibility gap strongly depend on the type of the miscibility gap and its position in the miscibility gaps.

Solid–liquid demixing will occur at low solvent (high polymer concentrations) and at high nonsolvent concentrations. At high polymer concentrations (case 1) crystallization takes place first giving rise to supramolecular assemblies such as spherulites. At low polymer concentrations (case 5) solid–liquid demixing can give rise to the formation of individual lamellae or immature spherulites.

For liquid–liquid demixing three types of phase separation mechanisms can be distinguished. At high polymer concentrations (between binodal and spinodal lines), phase separation takes place by nucleation and growth of a polymer poor phase and a spongy structure can be obtained (case 2). At intermediate polymer concentrations, spinodal-demixing processes give rise to bicontinuous network structures (case 3). At low polymer concentrations (between the binodal and the spinodal) phase separation takes place by nucleation and growth of a polymer rich phase and polymer spheres can be obtained (case 4).

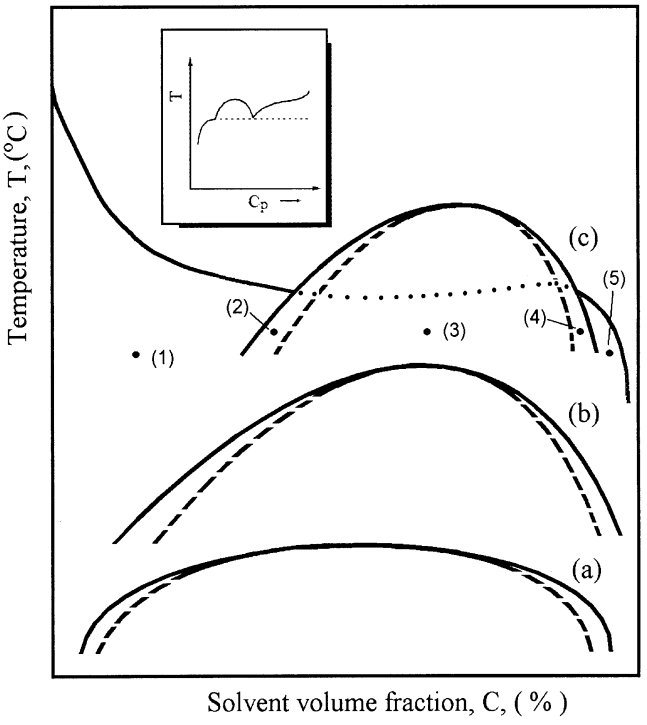


**Fig. 8** Schematic representation of the variation in the phase diagram with an increase of polymerization degree during CL polymerization. Both the liquid–liquid miscibility gap and solubility curve (the border of the solid–liquid miscibility gap) are shown independently. Initially, the solution is composed of small molecules of solvent, monomer and catalytic species. The dots at coordinates $(C_i,T_i)$ represent the reaction points. Since all points are above the liquid–liquid lines (a), the solutions are homogeneous. With polymerization the liquid–liquid lines gradually shift upward and towards the right side of the phase diagram. Two possible situations, namely when the liquid–liquid lines are located below (b) or overtake (c) the liquid–crystal lines are also illustrated. Depending on the position of the reaction points, these can be thrust inside the liquid–liquid miscibility gap or can remain in the solid–liquid miscibility gap. In the inset, a typical phase diagram of a thermally induced phase separation of a crystalline polymer in a poor solvent is presented

The efficiency of the catalytic system plays a determining role on the kinetics of polymerization also controlling the molecular weight of the polymer. Consequently, it is expected that the liquid–liquid line(s) will be shifted more or less on the phase diagram, according to the efficiency of the catalytic system. This means, that the reaction point, in coordinates $(C, T)$, may be located in different regions of the phase diagram by changing the catalytic components.

The influence of the efficiency of catalytic systems on the final morphology of PCA particles is schematically illustrated in Fig. 9. In almost all cases the obtained morphologies can be ascribed to a "cascade of phase transitions" [14]. Thus, the crystalization process is usually preceded by a liquid-lilke phase separation forming a polymer-rich phase. These polymer-rich domains

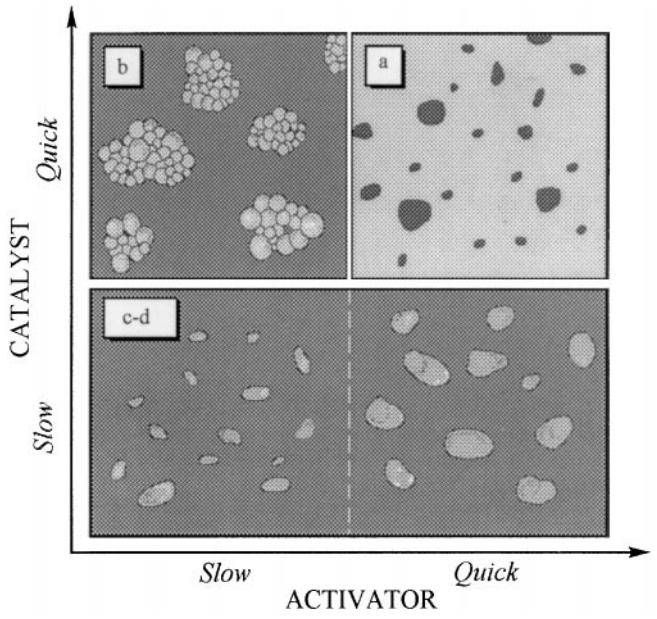


**Fig. 9** Schematic representation of the influence of the efficiency of the catalytic system on the morophology of the anionic PCA obtained in a nonpolar solvent: (a) large blocks formed by the coalescence of a large number of semiliquid droplets; (b) granules (fused agglomerates); (c) and (d) powders. ▒ polymer phase; ▓ solvent phase

constitute the preferable place where the chemical and physical processes will take place.

As is seen in Fig. 9 two main morphologies have been obtained, in accordance with the manner in which the growth of chains is started. When polymerization is started without any induction period ((a) quick–quick and (b) quick–slow activator/catalyst pairs), the polymer is obtained in the form of fused aggregates. Here depending on the nucleophilicity of caprolactam anions either granules (using catalysts which decrease the nucleophilicity of lactam anions) or large blocks (using the common catalysts) are formed. In these cases, liquid–liquid demixing takes place by nucleation and growth of a polymer rich phase, followed by crystallization of polymer-rich droplets. The morphological differences found concerning the individual particles which compose the PCA-granules (samples b1–b3 in Table 1) could also be explained taking into account the position of the reaction point with respect to liquid–liquid lines during polymerization. If it will remain all the time inside the metastable region, as in the case of PCA-IDI (sample $b_1$) smooth and almost spherical globules are obtained. Using more efficient activators (samples b2, and b3) the phase separation may start in the metastable region, but due to the fast chemical reactions, the reaction point can be thrust outside this region and the phase separation will proceed in the liquid–crystal region of the phase diagram.

In contrast, when initiation is the rate-determining step of polymerization and the chain-initiating species appear gradually and are able to act for a longer period in the reaction medium (slow–quick (c) and slow–slow (d) activator/catalyst pairs), powdery polycaproamides are obtained. In this case, spinodal decomposition, giving rise to interconnected network-type morphology, followed by rapid crystallization of the polymer-rich phase takes place within the already separated polymer-rich droplets. Using the slow catalysts, the only difference with respect to the catalyst efficiency seems to be the period of time until the occurrence of the phase separation, which is longer using slow catalysts (samples d1, and d2 in Table 1). In addition, no polymer is obtained at temperatures below 100 °C using slow–slow catalytic systems.

**Table 3** Influence of the catalytic system on the size distribution of PCA particles

| Code | Cat./Act. | Particles distribution | | | |
|---|---|---|---|---|---|
| | | $d_{50}$ [$\mu$m] | $-S_d$[a)] | GDS[b)] | $(1 + CV^{c)})^{d)}$ |
| b1 | RedAl/IDI | 277.49 | 1.88 | 1.97 | — |
| b11 | b1(grinded) | 12.57 | — | — | 1.64 |
| c1 | $Na/CO_2$ | 9.79 | 1.392 | 1.72 | — |
| c2 | Na/DICI | 51.56 | — | — | — |
| c3 | Na/DCCI | 71.19 | 2.17 | 1.68 | — |

*Abbreviations*: $S_d$, particle span distribution; GDS, geometrical standard deviation; CV, coefficient of variation; $\sigma$, standard deviation; $\bar{d}$, number-average particle diameter

[a)] Evaluated by the equation $S_d = (d_{10} - d_{90})/d_{50}$ [36].

[b)] Evaluated by the equation $GDS = (d_{84}/d_{16})^{1/2}$ [37].

where $d_i$ ($i = 10, 16, 50, 84, 90$) stands for the diameter corresponding to $i$% on the cumulative volume distribution (i.e. $i$% of the mass is in particles smaller than $d_i$).

[c)] Evaluated by the equation $CV = \sigma/\bar{d}$ ($\sigma = 8.12$, $\bar{d} = 12.57$ [10]).

[d)] According to ref. [37], $1 + CV \cong GDS$.

From Table 1 it appears that, the size of particles increases gradually with increase of the catalytic system efficiency (i.e. decreasing the time of polymer separation). This is not true because except for the powders, the granules (fused agglomerates) are composed of a large number of small, more or less spherical particles. Most likely, the blocks deposited on the walls of the flask are also formed by coalescence of a great number of semiliquid droplets. In other words, by increasing the efficiency of the catalytic system both the time of phase separation and average size of the individual particles decrease as is shown in Tables 1 and 3.

As is seen in Table 3, despite the wide range of particles' size their size distributions are close enough. However, the size distribution slightly increases with the increase of particle average size.

There is still a need to investigate the effect of other catalytic systems, solvents and temperatures on the final morphology of PCA particles. The use of other more powerful tools such as light-scattering and time-resolved X-ray scattering could provide supplementary information about the formation of PCA particles.

**Acknowledgements** The authors (and specially FD) thank Dr. Rudolf Puffr (Institute of Macromolecular Chemistry, Czech Academy of Science) for a stimulating discussion and for critically reading an earlier version of the manuscript.

## References

1. Biernacki P, Wlodarczyk M (1980) Eur Polym J 16:843–848
2. Chrzczonowicz S (1957) Zesz nauk Politech Lodz 5:65
3. Chrzczonowicz S, Wlodarczyk M, Ostaszewski B (1960) Makromol Chem 38:159–167
4. Sahler WA (1968) Br Patent 1.118.700, Chem Abstr 69:44630
5. Keizo U, Yusaku T, Fumimaro O (1968) Jap Patent 68 08833, Chem Abstr 69:36596
6. Biensam M, Braund P (1970) (a) German patent 1.964.533, Chem Abstr 73:67332; (b) German Pat 1.964.995, Chem Abstr 73:78175
7. Wolfers WP, Fransen PJ, Warnier JM (1972) Chem Abstr 77:115108
8. Kubanek V, Kralicek J, Moucha A (1976) Scientific Paper of the Prague Institute of Chemical Technology, Vol C24, pp 9–16
9. Kubanek V, Kralicek J, Kondelikova J (1977) Chem Abstr 87:400272
10. Vasiliu-Opera CL, Dan F (1996) J Appl Polym Sci 62:1517–1527
11. Vasiliu-Oprea CL, Dan F (1997) J Appl Polym Sci 64:2575–2583
12. Dan F, Vasiliu-Oprea CL (1998) J Appl Polym Sci 64: 231–243
13. McHugh AJ, Vrahopoulou E (1984) Macromolecules 17:2657–2663
14. Van de Witte P, Boorsma A, Esselbrugge H, Dijkstra PJ, Van den Berg JWA, Feijen J (1996) Macromolecules 29:212–219
15. Van de Witte P, Dijkstra PJ, Van den Berg JWA, Feijen J (1997) J Polym Sci, Polym Phys Ed 35:763–769
16. Burghardt WR (1989) Macromolecules 22:2482–2486
17. Stehlicek J, Labsky J, Sebenda J (1967) Collect Czech Chem Commun 29:56–59
18. Okay O, Gurun C (1992) J Appl Polym Sci 46:401–410
19. Szwarcz M (1974) In: Szwarcz M (ed) Ions and Ion Pairs in Organic Reactions, Vol 2. Wiley, New York, pp 424–426
20. Sekiguchi H (1984) In: Ivin KJ, Saegusa T (eds) Ring-Opening Polymerization, Vol 2. Elseview, London, p 833
21. Sebenda J (1989) In: Eastmond GC, Ledwith A, Russo S, Sigwalt P (eds) Comprehensive Polymer Science, Vol 3. Pergamon Press, Oxford, pp 511–530
22. Sebenda J (1991) In: Puffr R, Kubanek V (eds) Lactam-Based Polyamide, Vol 1. CRC Press, Boca Raton, FL, pp 29–73
23. (a) Veith CA, Cohen RE (1990) Polym Prepr (ACS Div Polym Chem) 31(1): 42–43; (b) Veith CA, Cohen RE (1991) Makromol Chem, Macromol Symp 42/43:241–258
24. Kubanek V (1985) In: Sodium Dihydrido-bis(2-methoxyethoxo)-aluminate (SDMA). A Versatile Organometallic Hydride. Academia, Prague, p 210
25. Komoto T, Iguchi M, Kanetsuna H, Kawai T (1970) Makromol Chem 135:145–164; Schaaf P, Lodz B, Wittman JC (1987) Polymer 28:193–200
26. Schaaf P, Lodz B, Wittman JC (1987) Polymer 28:193–200
27. Bar-Zakay S, Levy M, Vofsi D (1967) J Polym Sci A-I 5:965–974
28. Daer KM, Levendis YA (1992) J Appl Polym Sci 45:2061–2073
29. Stehlicek J, Sebenda J (1986) Eur Polym J 22:769–773
30. Heuvel HM, Huisman R, Lind KCJB (1976) J Polym Sci, Polym Phys Ed 14:921–940
31. Inoue T (1995) Prog Polym Sci, Vol 20. Elsevier, 119–153
32. Ohnaga T, Chen W, Inoue T (1994) Polymer 35:3774–3781
33. Shen C-S, Kyn T (1995) J Chem Phys 102:556–562
34. Yu Y-K, Wang X-Y, Taylor PL (1996) J Chem Phys 104:2725–2731
35. Chan KP, Rey DA (1996) Macromolecules 29:8934–8941
36. Akay G (1994) Polym Eng Sci 34:865–889
37. Paine AJ, Luymes W, McNulty J (1990) Macromolecules 23:3104–3109